Available online at www.sciencedirect.com
SCIENCE DIRECT
International Journal of Multiphase Flow 32 (2006) 159–182
International Journal of Multiphase Flow
www.elsevier.com/locate/ijmulflow

# Bubble growth in saturated pool boiling in water and surfactant solution

G. Hetsroni *, A. Mosyak, E. Pogrebnyak, I. Sher, Z. Segal

*Department of Mechanical Engineering, Technion—Israel Institute of Technology, 32000 Haifa, Israel*

Received 10 February 2005; received in revised form 16 October 2005

**Abstract**

The presence of surfactant additives in water was found to enhance the boiling heat transfer significantly. The objective of the present investigation is to compare the bubble growth in water to that of a surfactant solution with negligible environmental impact. The study was conducted at two values of heat fluxes to clarify the effect of the heat flux on the dynamics of bubble nucleation. The bubble growth under condition of pool boiling in water and non-ionic surfactant solution was studied using high speed video technique. The bubble generation was studied on a horizontal flat surface; and the natural roughness of the surface was used to produce the bubbles.

We did a quantitative analysis of single bubble growth, in saturated nucleate pool boiling of water, with constant wall heat flux $q = 10$ and 50 kW/m$^2$. The captured images showed that the bubble shape is close to axially-symmetric and vertically non-symmetric. At heat flux of $q = 10$ kW/m$^2$ the life-time and the volume of bubble growth-rate in surfactant solution did not differ significantly from those of water. The time behavior of the contact angle of bubble growing in surfactant solution is qualitatively similar to that of water.

At a heat flux of $q = 50$ kW/m$^2$, boiling in surfactant solution, when compared with that of pure water, was observed to be more vigorous. Surfactant promotes activation of nucleation sites; the bubbles appeared in a cluster mode; the life-time of each bubble in the cluster is shorter than that of a single water bubble. The detachment diameter of water bubble increases with increasing heat flux, whereas analysis of bubble growth in surfactant solution reveals the opposite effect: the detachment diameter of the bubble decreases with increasing heat flux.


*Keywords:* Pool boiling; Heat transfer; Surfactant; Bubble dynamics; Contact angle

## 1. Introduction

Boiling heat transfer is employed in many industrial processes, either to generate vapor or because of its effectiveness in cooling. The applications cover many fluids and mixtures. Fully quantitative predictive models

* Corresponding author. Tel.: +972 48 292058; fax: +972 48 238101.
*E-mail address:* hetsroni@tx.technion.ac.il (G. Hetsroni).

0301-9322/$ - see front matter © 2005 Elsevier Ltd. All rights reserved.
doi:10.1016/j.ijmultiphaseflow.2005.10.002

are still under development, since they require information about heat transfer mechanisms derived from theoretical models and from detailed experiments on bubble dynamics.

Many criteria for bubble shape or bubble detachment diameter were considered for describing the dynamic process of bubble growth. The distinct feature of bubble dynamics is that contact angle deviates from the static value due to the rapidity of the growth. The well-known Fritz equation (1936) predicts bubble departure diameter for contact angle of 48°. This agrees well with the experimental data at atmospheric pressure. Hsu and Graham (1961) assumed a contact angle of 53.1°. Han and Griffith (1965) presented a theory and experimental results of bubble growth of pool boiling at low heat flux. Bubble departure was considered by the authors and it was found that the Fritz relation works as the non-equilibrium bubble contact angle. Most of the previous research on single bubble growth has been performed using a constant wall heat flux created by heating a metallic block beneath the bubble (Staniszewski, 1959; Han and Griffith, 1965; Cole and Shulman, 1966; Van Stralen, 1966). The effect of pressure for contact angle of 48° was accounted by Cole and Shulman (1966).

Analytical analyses for the growth of a single bubble have been performed for simple geometrical shapes, using a simplified heat transfer model. Plesset and Zwick (1954) solved the problem by considering the heat transfer through the bubble interface in a uniformly superheated fluid. The bubble growth equation was obtained from the conduction through the thermal boundary layer around the bubble. The interface cooling effect was reported also by Zuber (1961) and Mikic et al. (1970).

Zeng et al. (1993) proposed that the dominant forces leading to bubble detachment would be the unsteady growth force and buoyancy force. In order to derive an accurate detachment criterion from a force balance, all forces should be accurately known. If a mechanism is not known precisely, approximate expressions, one or two fitted parameters and comparison with experiments, might offer a solution. Such fitting procedures have indeed been applied (Klausner et al., 1993; Mei et al., 1995a; Helden et al., 1995).

Mei et al. (1995b) developed a numerical model for vapor bubble growth in saturated pool boiling and demonstrated that the bubble growth rate is reduced due to the resulting temperature gradients beneath the nucleation site. Thorncroft et al. (1998) carried out experimental investigation of bubble growth and detachment in vertical up flow and down flow boiling. They observed that the growth data fit a power low ranging from about $t^{0.33}$ to $t^{0.5}$, where $t$ is the time. The models of bubble growth and correlations for the bubble radius are discussed by Thorncroft et al. (2001).

Robinson and Judd (2001) considered four regions of bubble growth: surface tension controlled region, transition domain, inertial controlled growth and heat transfer controlled growth. A theory has been developed that is able to accommodate both spatial and temporal variations in the temperature and velocity fields in the liquid surrounding the bubble as it grows. Overall agreement between the theory and experimental data is very good. Bubble growth and variation of bubble lifetime and size with flow rate, subcooling, heat flux and pressure were examined by Prodanovic et al. (2002).

Nucleate pool boiling experiments with constant wall temperature were performed by Lee et al. (2003) using R11 and R113 for saturated boiling conditions. The geometry of the bubble was obtained from the images. The bubble growth rate was proportional to $t^{0.2}$, which was slower than the growth rate proposed in previous studies. Detachment of a vapor bubble from a plane, solid wall has been studied theoretically by Geld (2004). The vapor–liquid interface shape has been approximated by that of a truncated sphere. The forces related to gravity and surface energy densities were found to be major contributors to departure time.

There has been extensive research and development in enhanced boiling heat transfer. Among the different enhancement techniques investigated, the use of surfactant additives in water has been found to change boiling phenomenon drastically. It is important to understand the effects of surfactants on boiling heat transfer and bubble dynamics. Surfactants are essentially low-molecular weight chemical compounds, with molecules that consist of a water-soluble (hydrophilic) and a water insoluble (hydrophobic) part. Depending upon the nature of the hydrophilic head group, surfactants are primarily classified as anionic, non-ionic, and cationic. Depending on the ionic character of the surfactant, the molecular weights and surface tension depression in aqueous solutions are generally greater in the order of non-ionic > anionic > cationic.

Small concentrations of surfactant in water lower the solution's surface tension considerable, and the level of reduction depends on the amount and type of surfactant present in solution. In general, with increasing additive concentration the surface tension $\sigma$ decreases appreciably. With increasing concentration, an asymp-

totic limit of $\sigma$ is obtained at the critical micelle concentration (cmc) of surfactant, which is characterized by the formation of colloid-sized clusters or aggregates of monomers called micelles. The cmc is a direct measure of the effectiveness of a surfactant to reduce the solvent's surface tension, and it depends upon the surfactant's chemistry and ionic structure (Rosen, 1989). The surface tension of aqueous surfactant solutions has also been found to be temperature dependent. Elevated temperatures cause a decrease in surface tension.

The study of the saturated pool boiling of a surfactant solution shows a significant enhancement of the heat transfer (Wasekar and Manglik, 2000; Hetsroni et al., 2001; Sher and Hetsroni, 2002; Hetsroni et al., 2004a,b). Wasekar and Manglik (1999), Manglik et al. (2001), Yang and Maa (2003) published the comprehensive reviews on the heat transfer in nucleate pool boiling of aqueous surfactants and polymeric solutions.

The rheological and diffusion effect on bubble growth was considered for drag reducing polymer solutions. Kotchaphakdee and Williams (1970) observed that the vapor bubbles produced in the polymer solutions were smaller than those produced in the pure solvent. Paul and Abdel-Khalik (1984) showed that compared to pure water boiling at the same heat flux, the polymer solutions have slightly smaller average bubble departure diameters. Effects of elastic viscosity and diffusion resistance during the growth of vapor bubbles in a polymer solution were investigated theoretically by Shulman and Levitsky (1996). To the best knowledge of the present authors there are only a few publications considering bubble dynamics in drag reducing surfactant solutions.

Boiling incipience and vapor bubble growth dynamics in aqueous surfactant solutions were studied using high speed photography by Wu and Yang (1992). The bubble growth period was observed to increase slightly, while the waiting period and the time interval between two consecutive bubbles were reduced drastically. The experimental results of bubble dynamics for pure water and 100 ppm SDS solution at relatively low heat flux of 23 kW/m$^2$ were presented by Yang and Maa (2003). It was shown that the departure diameter decreases considerably with an addition of surfactant. Zhang and Manglik (2004) reported that the heat transfer in saturated boiling of aqueous cationic surfactant solutions was enhanced considerably, and it generally increased with increasing heat flux. However, they observed that bubble dynamics is different in boiling of CTAB and Ethoquard 18/25 surfactant solutions. They assumed that such a different behavior may be attributed to surface wettability characteristics (the measured contact angle is different for CTAB and Ethoquard 18/25 surfactant solutions).

Unfortunately, these surfactants are not suited for industrial systems because of degradation and because of their environmental impact. That is why we have begun to study an enhancement of boiling by alkyl polyglucosides. They are non-ionic surfactants with negligible environmental impact (von Rybinski and Hill, 1998). Their production from the renewable resources glucose and fatty alcohol and their ultimate biodegradation is an example for a closed cycle. We used non-ionic alkyl (8–16) Glycoside for our experiments with concentration of $C = 600$ ppm. The objective of the present investigation is to compare the bubble growth in water and in the surfactant solution with negligible environmental impact. The study was conducted at two values of heat fluxes to clarify the effect of heat flux on the dynamics of bubble nucleation.

## 2. Experimental

### 2.1. Rheological properties of surfactant solution

The solution was prepared by dissolving the surfactant (52% active substance and 48% water) in deionized water, with gentle stirring over a period of a one-day. The measurements of the physical properties were carried out at the Department of Chemical Engineering, Ohio State University (Hetsroni et al., 2004b).

The surface tension data were obtained by using a Surface Tensiometer System. This system measures the surface tension within the body of a test fluid by blowing a bubble of gas through two probes of different diameters inside the fluid. The measurements of surface tension were carried out over a range of temperature from 300 to 368 K with standard deviation of 2%. The results are presented by Hetsroni et al. (2004b).

An increase in the surfactant concentration up to $C = 300$ ppm (parts per million weight) leads to significant decrease in the surface tension, whereas the surface tension is almost independent of concentration in the range $300 \leqslant C \leqslant 1200$ ppm. The $\sigma$–$T$ characteristics at different concentration of surfactant solutions were used to obtain the critical micelle concentration (cmc). At low concentration, surfactant molecules arrange themselves at the interface in the form of monomers with their hydrophilic part inside the water and the

hydrophobic part away from the interface. This results in an appreciable reduction in the surface tension at the interface. This process continues with increasing concentrations till cmc is reached, at which point no more molecules can be arranged at the interface (Rosen, 1989). In all cases, an increase in a liquid temperature leads to a decrease in the surface tension. The standard methods of measurement of surface tension cannot be used when the temperature of surfactant solution reaches the saturation temperature, $T_s$. That is why the cmc point was obtained at temperatures less than $t_s$. For example the cmc values of surfactants considered in study by Manglik et al. (2001) were obtained at $T = 298$ K. Our results showed that in the range of solutions temperature from 300 to 368 K the cmc point was reached at $C = 300$ ppm.

### 2.2. Apparatus

The apparatus for studying the bubble growth is depicted in Fig. 1a. The objective of these experiments was to study bubbles growing in a fixed position of the heater. The vessel was filled with the investigated liquid (water or surfactant solution) where a saturation temperature of the liquid was maintained at atmospheric pressure. The bubble generation was studied on a horizontal stainless steel foil of 0.05 mm thickness. The

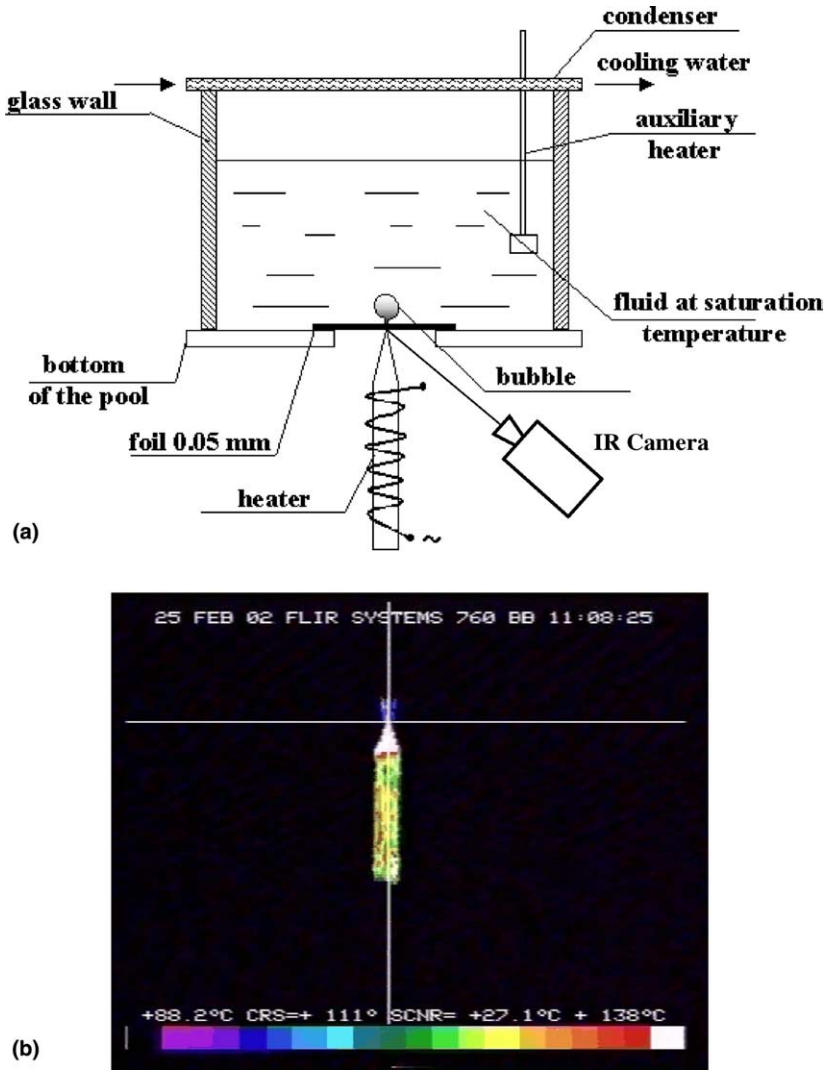


Fig. 1. Experimental facility and calibration procedure: (a) apparatus, (b) IR image.

Table 1
Roughness parameters

| Type of boiling surface | Maximum peak-to-valley height $R_{max}$ (μm) | Average roughness $R_{av}$ (μm) |
|---|---|---|
| Before boiling | 1.32 | 0.100 |
| After boiling | 5.40 | 0.670 |

natural roughness of the surface was used to produce bubbles. The roughness parameters measured by Profile measuring instrument are given in Table 1. The cone-shaped calibrated heater was moved up to contact with lower surface of the foil. The heater and the surface were covered by black color. The contact pressure was regulated by special traverse mechanism and controlled by a dynamometer.

The growth of the bubbles and the bubble motion near the heated surface were recorded by a high-speed video camera with recording rate up to 10,000 frames per second. The playback speed can be varied from a single frame to 25 frames per second.

### 2.3. Calibration

The fact that a bubble can be generated at a controllable location can be attributed to the specially designed cone-shaped heater, because it can provide a highly localized heating at a specific location of contact with the stainless steel foil. Constant heat flux was achieved by supplying controlled AC power to the heater. Since the heat flux transferred from the heater to boiling fluid through the foil cannot be known a priori, it must be found by calibration tests. The calibration process was conducted for saturated water boiling in the vessel. The heater was moved toward the foil to touch it. The displacement was controlled by a micro-meter. Then the water into the vessel was heated up to saturation temperature and the controlled power was applied to the heater. The bubbles were generated at a location of contact the conic part of the heater with the stainless steel foil. At this point the surface temperature was measured by infrared radiometer (Fig. 1a and b). The minimum detectable temperature difference of the radiometer is 0.1 K. Through calibration, the radiometer is very accurate in a narrow temperature range giving typical noise equivalent temperature difference (NETD), which is less than 0.2 K (with image average less than 0.05 K). A typical horizontal resolution is 1.8 mrad or 256 pixel/line. The heat flux was defined by using boiling curve for saturated water pool boiling. The calibration process was conducted at the same indication of the micro-meter for different power applied to the heater. The standard deviation of the heat flux defined in such a way was 14%.

### 2.4. Experimental procedure

The heating surface was cleaned routinely before and after each set of three data points with a sequence of operations involving application of constantan cleaner and washing with hot tap water and deionized water. Only a soft sponge and absorbent paper tissues contacted the stainless steel foil, which remained smooth and completely wettable.

During a typical run, the boiler was loaded with 1500 ml of liquid to bring the surface to a level 70–80 mm above the heater. It should be noted that the desorption of the dissolved gas forms bubbles of gas and a limited amount of bubbles containing gas–water vapor mixture. As a result, boiling incipience occurred at the channel wall temperature below that of saturation temperature. As the surface temperature of the cannel approaches the saturation temperature the effect of dissolved gases vanishes. Degassed water and surfactant solution were used in the present study. The data were obtained when the channel wall temperature exceeded the saturation temperature. To avoid effect of dissolved gases on bubble formation, experiments were carried out after 1 h, when the saturated pool boiling began. Surfactant solutions were replaced with fresh samples after three runs. This precaution was taken in order to minimize changes in solution properties, which might have occurred at high temperature due to evaporation over long periods of time.

While renewing the liquid, the heater surface was examined. No visible deposits formed under the test conditions, based on observations in the test runs and after draining the boiler. Room temperature was maintained at 23 °C, so that heat losses from the boiler would be nearly constant in all runs.

## 3. Results

### 3.1. Verification of the method

Fig. 2 shows a comparison of time dependence of the equivalent bubble radius obtained under condition of saturated pool boiling of water in the present work, with previous saturated pool boiling data. The equivalent bubble radius is radius of a sphere, whose volume is equivalent to the volume of actual bubble. The errors of the dimension measurement will propagate into the calculation of the equivalent radius. Dimensions of a bubble were measured by counting the number of pixels in a symmetric bubble image. A physical dimension of 1mm corresponds to 30 pixels, i.e. 1 pixel in the image corresponds to 0.033 mm. The captured images for surfactant solution were not clear and the bubble dimensions could be measured with maximum error of $\pm 2$ pixel, whereas clear images for water could be measured with the error of $\pm 1$ pixel. The images were taken with the time resolution of 1 ms.

In the previous experiments, water (Staniszewski, 1959; Han and Griffith, 1965), and *n*-pentane (Cole and Shulman, 1966) were used as working fluids. A constant heat flux was applied at the heating surface. The solid line represents dependence $R \sim t^{1/2}$. Plesset and Zwick (1954) assumed a uniformly superheated thermal boundary layer around a spherical bubble and predicted a $R \sim t^{1/2}$ asymptotic growth rate. Other predictions that modified the effective heat transfer area (Van Stralen, 1966) and the non-uniform temperature field around the bubble (Mikic et al., 1970) still gave an asymptotic growth rate of approximately $R \sim t^{1/2}$. Since most previous results have been for a spherical bubble, we used in the present comparison the equivalent radius of a sphere with the same volume. To evaluate the equivalent radius of the actual bubble the coordinate of the bubble interface were measured and the volume was calculated by the integration with the interfacial coordinate. The present results show the same growth rate proportional to $t^{1/2}$, after time interval of 1 ms.

### 3.2. Dynamics of bubble nucleation

The nucleate pool boiling experiments were conducted under atmospheric pressure at saturation temperature. When the energy input from the heater reached a value for the onset of bubble generation, single bubbles could be observed clearly, stably and repeatedly on the foil surface. The bubble growth was measured under constant heat flux condition at $q = 10$ and 50 kW/m$^2$. From the video, we can see that bubble grew rapidly

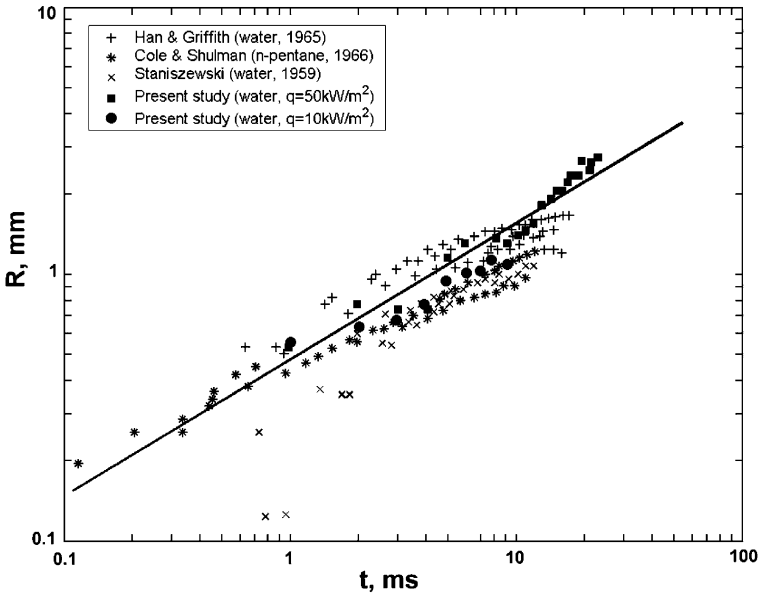


Fig. 2. Dependence of water bubble radius on time.

until reaching its maximum size, and then departed from the heated surface. Only one nucleation site was observed. The size and the frequency of the single bubble appearance changed with an increase in the heat flux and after certain value of heat flux a coalescence of the bubbles occurred. This value is different for water and surfactant solution. Whereas the single bubbles of water were observed at $q = 10$ and 50 kW/m$^2$ for boiling of surfactant solution they were observed only at $q = 10$ kW/m$^2$.

*3.2.1. Bubble growth at q = 10 kW/m$^2$*

For both water and surfactant boiling it is the region, in which bubbles were growing and detaching without significant influence from neighboring bubbles. In order to characterize single bubble dynamics quantitatively, the bubble size in each frame of the digitalized video was obtained using a Matlab Program (the details are presented in Appendix A). Approximately 100 bubbles from each film were analyzed. Upon analyzing bubbles from inception to lift-of from the surface, a significant difference in bubble size and lifetimes for bubbles on the same film (same experimental conditions) has been observed. This has been attributed to the fact that bubbles: (i) were initiated from different nucleation sites and (ii) experienced varying local temporal and velocity fields. It was therefore necessary to establish a mechanism for identifying typical bubbles from each film. We employed the methodology suggested by Paul and Abdel-Khalik (1984). Using films of each experimental series, the diameter for each bubble leaving the heated surface has been measured. The experiments were repeated and typically 5–6 series that were conducted at the same heat flux. By taking these measurements over a known period of time, for each series that contain 100 frames, a distribution of bubble diameters was obtained. From histogram that represents actual experimental data for each series the bubble detachment diameter corresponding to the maximum probability distribution was determined. The arithmetic mean diameter of all series was used as a typical bubble parameter. In the present study, analysis was carried out for bubbles, which departure diameter did not exceed 20% from the arithmetic mean.

Figs. 3 and 4 show the actual images of bubbles growth (marked by a white square) for water and surfactant solution. Figs. 5 and 6 show calculated axi-symmetrical bubble of water and surfactant. As the bubble grows, its shape is changed to ovoid necking at the foil surface. Soon after the neck appeared, the bubble center accelerated upward. The bubble is detached when the buoyant force just overcomes the surface tension.

*3.2.2. Time variation of bubble size*

Fig. 7 shows comparison between experimental results of time variation of bubble volume for water and 600 ppm alkyl (8–16) surfactant solution. For time interval $t = 1$–10 ms no distinct features were observed between dependence of bubble volume on time, under conditions of pool boiling of water and surfactant solution. At $t > 10$ ms the water bubble growth is faster than that of surfactant solution. In the previous section (Section 3.1) it was shown for water boiling that asymptotic growth rate is approximately $t^{1/2}$. According to Thorncroft et al. (1998) such a behavior can be attributed to the diffusion controlled growth in saturated boiling. In this stage the rate of bubble expansion is considered to be limited by the rate at which liquid is evaporated into the bubble. It is dictated by the rate of heat transfer by conduction through the liquid (Robinson and Judd, 2001). The decrease in the growth rate of surfactant solution at $t > 10$ ms suggests that in the heat controlled region, the behavior of bubble dynamics is different from that of water even for low heat flux. While boiling of pure liquids is influenced by surface tension, thermal conductivity, boiling of surfactants with reduced surface tension is also influenced by mass diffusion and Marangoni effect. In Figs. 8 and 9 we compare the time behavior of maximum bubble diameter and the maximum bubble height of water and surfactant bubble. These values increase with time for both fluids. It will be shown in the next section that the shape of the vapor bubble in water differs from that in surfactant solution.

*3.2.3. Dynamic contact angle histories*

In the present study, the liquid–vapor interface had an ovoid shape with its foot attached to a plane wall. Bubble shape is the governing factor in mechanism of bubble growth and motion in nucleate pool boiling. The rapidity of the bubble growth allows the contact angle to deviate from the static value. In the present study, the contact angle was calculated from bubble images taken at a time interval of 1 ms. For each image the line determining the boundary of the bubble in the $x$–$y$ plane was described by a function $x = X(y)$. The contact angle was defined as $dx/dy$ at $y = 0$. The maximum uncertainty of the contact angle is 16% for the first image

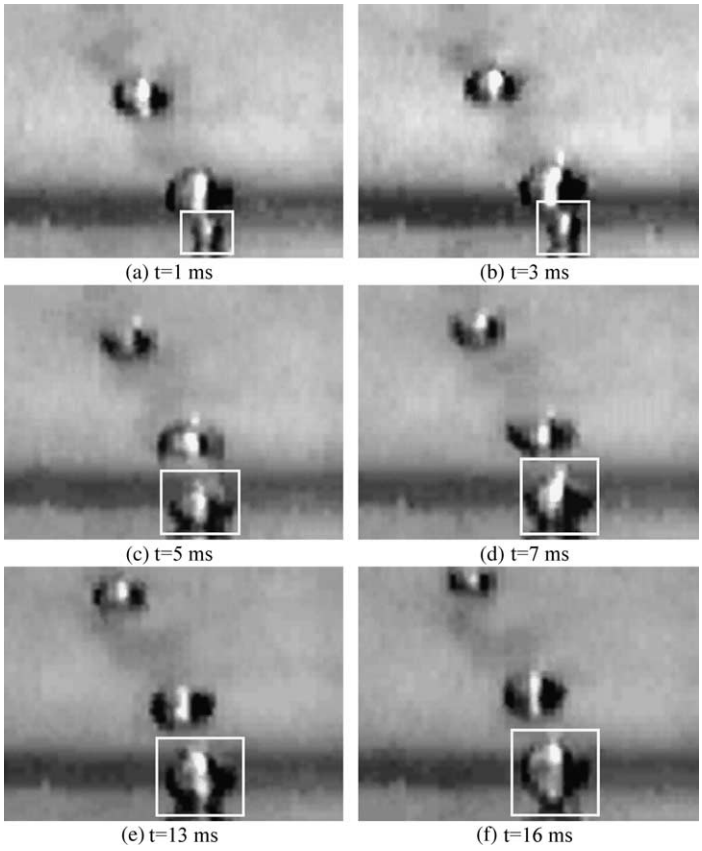


Fig. 3. Boiling of water, $q = 10\ \mathrm{kW/m^2}$.

that showed the smallest bubble, and 9% for the image before bubble departure. In making the comparisons between experiments it should be stressed that contact angles and measured delay times were used. Neither of these quantities was constant from bubble to bubble. This randomness has been observed before in boiling process by Han and Griffith (1965) and is apparently inherent to it. One may conclude that large fluctuations in bubble history resulted from relatively small turbulent fluctuations in the temperature conditions around the bubbles. An exact prediction of what is going to occur in such a situation does not appear to be possible. In making the comparisons between experiments the arithmetic mean obtained from 100 measurements was used as a typical contact angle.

Fig. 10 shows time behavior of contact angle for water and surfactant solution. For both liquids at $t = 1$ ms the contact angle is approximately of $\theta = 60°$. Throughout bubble growth this value decreases approximately up to 41° and up to 51° for water and surfactant solution, respectively. For water the dynamic effect of bubble growth rate on contact angle agrees quite well with data reported by Cole and Shulman (1966), Han and Griffith (1965) and Fritz and Ende (1936). The time behavior of contact angle of bubble growing in surfactant solution is qualitatively similar to that of water.

In the model for predicting the growth and detachment of a vapor bubble suggested by Mei et al. (1995a) the liquid microlayer between the vapor bubble and the solid heating surface was assumed to have a simple wedge shape with an angle $\theta$. During the bubble growth, the dome had approximately a spherical shape with a radius $R(t)$. The radius of the wedge-shaped interface was denoted by $R_{\mathrm{foot}}$, and the shape parameter was denoted by $C = R(t)/R_{\mathrm{foot}}$. Mei et al. (1995a) assumed that $C$ is independent of time, for simplicity. In the present study dependence of the shape parameter on time was determined experimentally. Fig. 11a and b shows experimental data for boiling of water and surfactant solution, as the shape parameter $C_{10} = d_{\mathrm{foot}}/D$ vs. time for $q = 10\ \mathrm{kW/m^2}$. For water boiling, Fig. 11a, the shape parameter decreases with time. Experiments

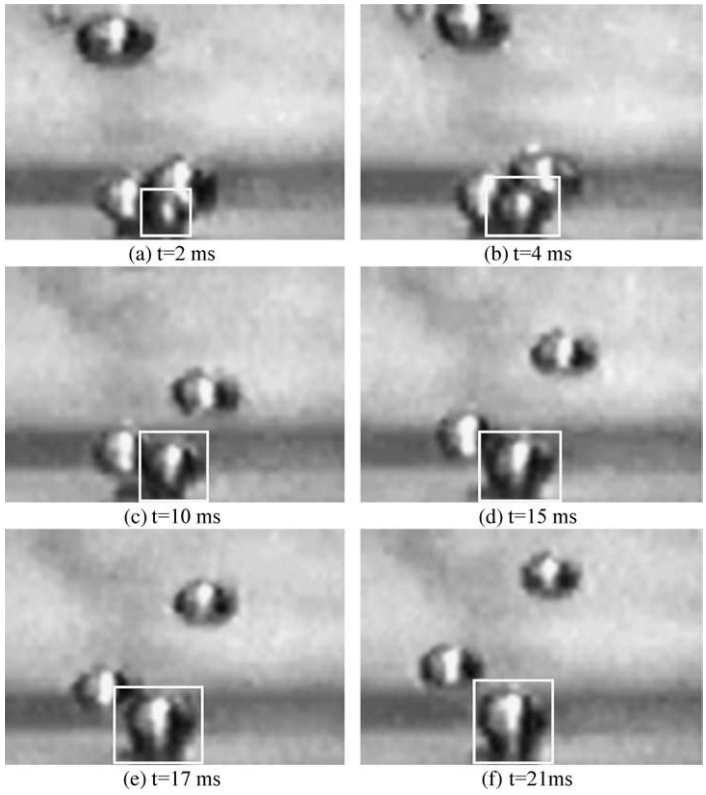


Fig. 4. Boiling of alkyl (8–16), $q = 10$ kW/m$^2$.

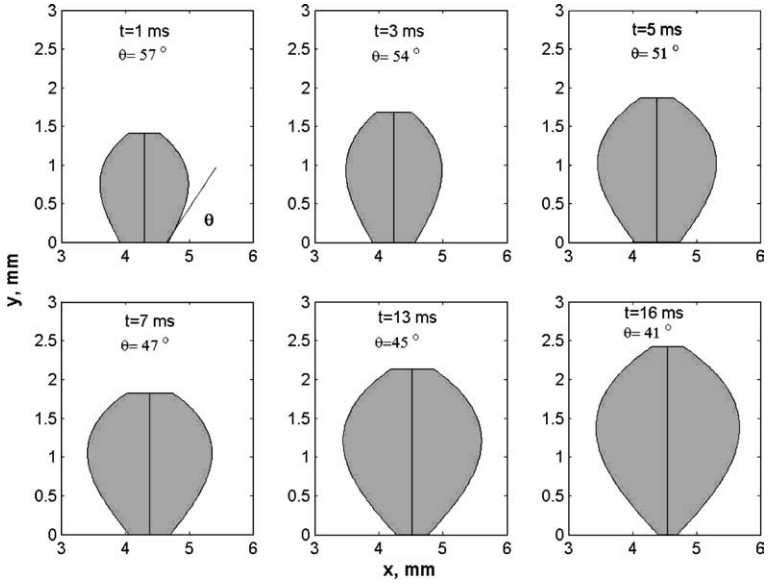


Fig. 5. Computed results, water, $q = 10$ kW/m$^2$.

in water were carried out at Jacob number of about $Ja = 6$, and the average value of parameter was about $C_{10} = 0.4$. According to the correlation suggested by Mei et al. (1995a), the shape parameter at $Ja = 6$ is $C = 0.5$, which agrees reasonable well with the average value obtained in our experiments. For boiling of

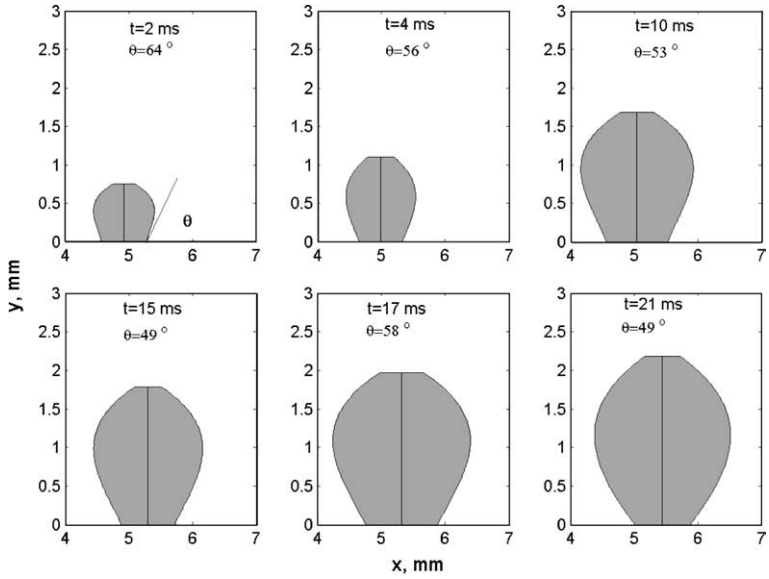


Fig. 6. Computed results, alkyl (8–16), $q = 10\ \mathrm{kW/m^2}$.

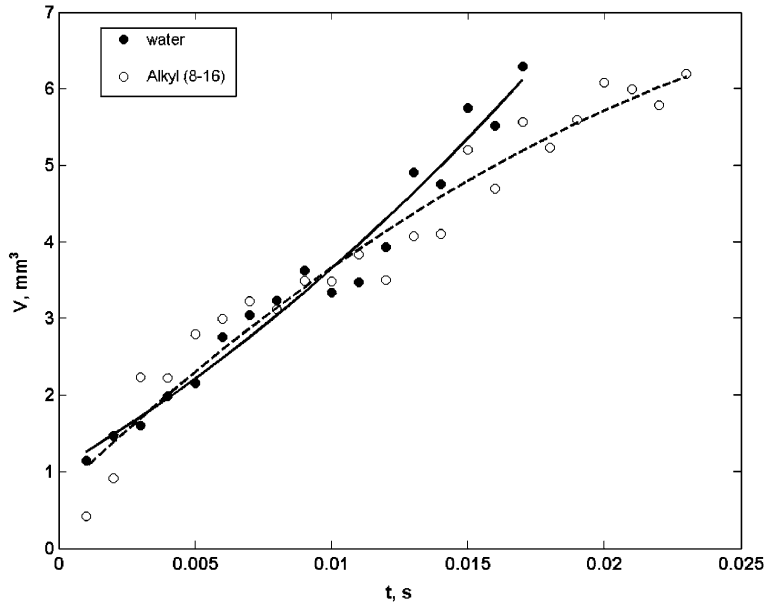


Fig. 7. Dependence of bubble volume on time, $q = 10\ \mathrm{kW/m^2}$.

surfactant solution, Fig. 11b, the time behavior of the shape parameter is quite different. At time $t > 0.005$ s the value of $C_{10}$ almost did not change.

Another determination of the bubble shape was presented by Geld (2004). It is the ratio of the diameter of the bubble foot at a given time, $d_{\mathrm{foot}}$, to its initial value $d_{\mathrm{foot0}}$. Fig. 12a and b shows dependence $d_{\mathrm{foot}}/d_{\mathrm{foot0}}$ on time. For water, Fig. 12a, this parameter decreases with time. Such a behavior is in agreement with the prediction by Geld (2004). For surfactant solution (Fig. 12b), $d_{\mathrm{foot}}/d_{\mathrm{foot0}}$ increases with time. Consequently, the local temperature of the solid surface directly beneath the bubble foot, will decrease with time, because the local rate of energy removal due to the bubble growth is typically much larger than that added. As the local

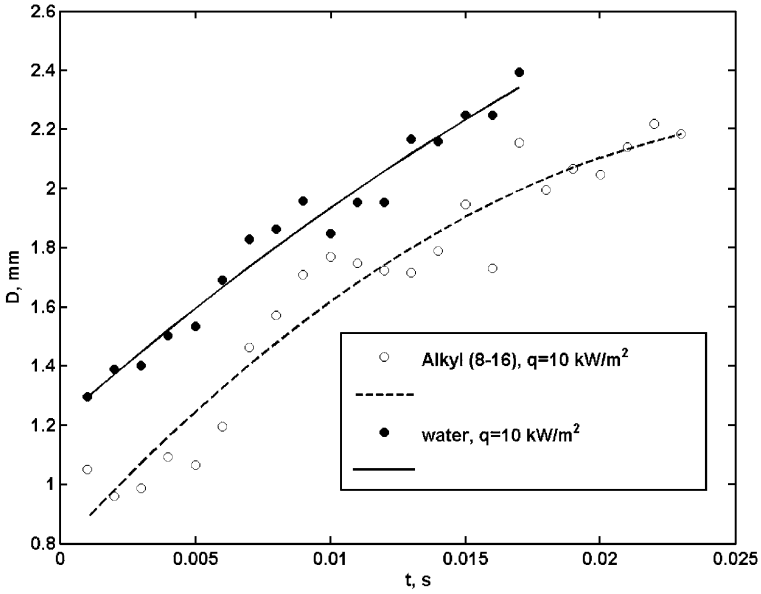


Fig. 8. Time variation of bubble diameter, $q = 10\ \mathrm{kW/m^2}$.

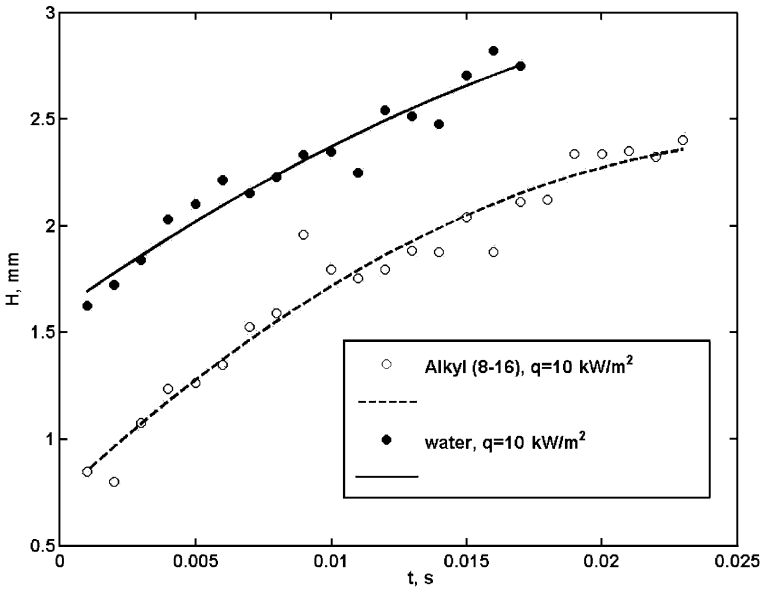


Fig. 9. Time variation of bubble height, $q = 10\ \mathrm{kW/m^2}$.

solid wall temperature decreases with time the temperature gradient across the microlayer is reduced, the rate of energy transferred to the bubble reduces, and the bubble growth rate decreases.

*3.2.4. Bubble growth at q = 50 kW/m²*

Fig. 13 shows the images of water bubble growth. Single bubble appeared and grew on the heated surface, no bubble coalescence was observed. A different situation arises with the bubble growth in surfactant solution. Fig. 14 shows the typical image of bubbles originated in 600 ppm (alkyl (8–16)) surfactant solution. The figure presents a cluster of small bubbles, which rise in the neighborhood of the cavity. Boiling in surfactant solution,

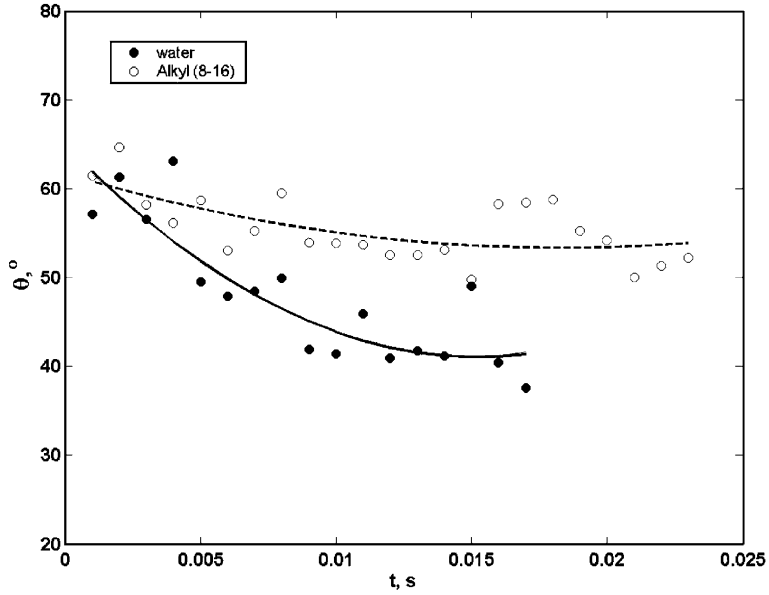


Fig. 10. Dependence of contact angle on time, $q = 10\ \mathrm{kW/m^2}$.

when compared with that in pure water, was observed to be more vigorous. Surfactant solution promotes activation of nucleation sites in a clustered mode. This may be due to the retarded bubble coalescence caused by the Marangoni effect and the effect of elasticity described by Yang and Maa (2003). The cluster contains a number of small bubbles, the location of nucleation sites and time behavior of each cannot be traced exactly. A surfactant solution cannot be expected to boil in the same way as a pure liquid even with exactly the same equilibrium surface tension value and other physical properties.

The life-time of each bubble in a cluster is shorter than that of single water bubble. The average growth time of a bubble depends on the forces acting on the growing bubble. Due to rheological forces, the average growth time in surfactant solution is considerably shorter than that in water. Our results obtained at $q = 50\ \mathrm{kW/m^2}$ agree qualitatively with those reported by Paul and Abdel-Khalik (1984) for bubble dynamics during boiling along the heated surface of the platinum wire at heat flux $q = 35.8\ \mathrm{kW/m^2}$. For images presented in Figs. 13 and 14, the life-time of a single water bubble is of 21 ms, whereas it is about 9 ms for surfactant solution.

Dependence of bubble volume on time is presented in Fig. 15. Analysis of the curves in Fig. 15 shows that the growth of bubbles in surfactant solution occurs slower than in water. With heating from below the surfactant-enriched phase, which has a higher density, finds itself near the heating surface, as a result of which the growth of vapor bubbles occurs under conditions of deficit of the volatile component.

The time dependence of bubble diameter and bubble height is plotted in Figs. 16 and 17. Comparison of data presented in Figs. 16 and 17 to those presented in Figs. 8 and 9 displays that the detachment diameter and height of water bubble increases with increasing heat flux, whereas the detachment diameter and height of bubble growing in surfactant solution decreases with increasing heat flux. Increase in detachment water bubble diameter with increase in heat flux agrees with experimental results reported by Cole and Shulman (1966) and Van Stralen (1966) using water as boiling liquid. This phenomenon can be connected to increase in the Jacob number, with increase in heat flux. The Jacob number is $Ja = \rho_{\mathrm{L}} C_{p\mathrm{L}} \Delta T_{\mathrm{sat}} / \rho_{\mathrm{G}} h_{\mathrm{LG}}$ where $C_{p\mathrm{L}}$ is the specific heat of the liquid, $\rho_{\mathrm{L}}$ and $\rho_{\mathrm{G}}$ is liquid and vapor density, $\Delta t_{\mathrm{sat}} = t_{\mathrm{W}} - t_{\mathrm{S}}$ is the difference between wall temperature and saturation temperature, $h_{\mathrm{LG}}$ is the latent heat of vaporization. The analysis performed for the governing equations and boundary conditions by Mei et al. (1995a,b) showed that the Jacob number is the most important parameter affecting bubble growth in Newtonian liquid. An increase in the Jacob number leads to an increase in the detachment bubble diameter.

For non-Newtonian fluids the boiling is accompanied by manifestation of a number of specific factors. The role of rheological effects and diffusion transport during the expansion of bubbles in such solutions should be

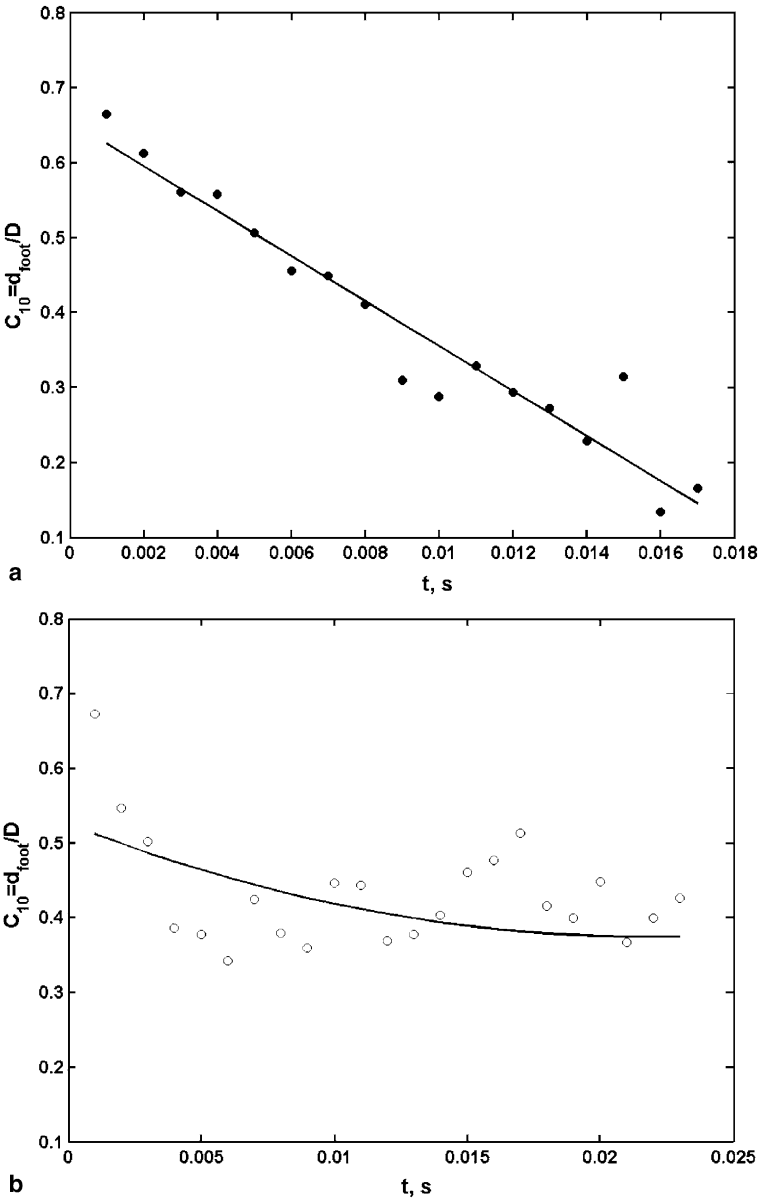


Fig. 11. Time variation of shape parameter, $q = 10\ \mathrm{kW/m^2}$: (a) water, (b) alkyl (8–16).

taken into account. Shulman and Levitsky (1996) reported that increase in the diffusion resistance leads to a decrease in the Jacob number and the rate of the growth of bubbles in a polymer solution is always smaller than in a single component fluid. We assume that at high heat flux diffusion retards the growth of vapor bubbles also in surfactant solution.

Fig. 18 shows the dependence of the shape parameter, $C_{50} = d_{foot}/D$, on time, $t$, for bubble that growth during boiling in water. The Jacob number was about $Ja = 10$. Fig. 19 displays comparison between data presented in Figs. 18 and 11a. The relation of the shape parameter $C_{50}$ obtained at heat flux $q = 50\ \mathrm{kW/m^2}$ to the shape parameter $C_{10}$ obtained at heat flux $q = 10\ \mathrm{kW/m^2}$ is plotted in Fig. 19. Increase in shape parameter with increase in the Jacob number agrees with prediction by Mei et al. (1995a) Fig. 20 shows that dependence $\theta/\theta_0$ on time for water boiling decreases with time. Such a behavior is in agreement with prediction by Geld (2004). Fig. 21 shows dependence $d_{foot}/d_{foot0}$ on time. Up to time $t = 0.005$ s this parameter increases with

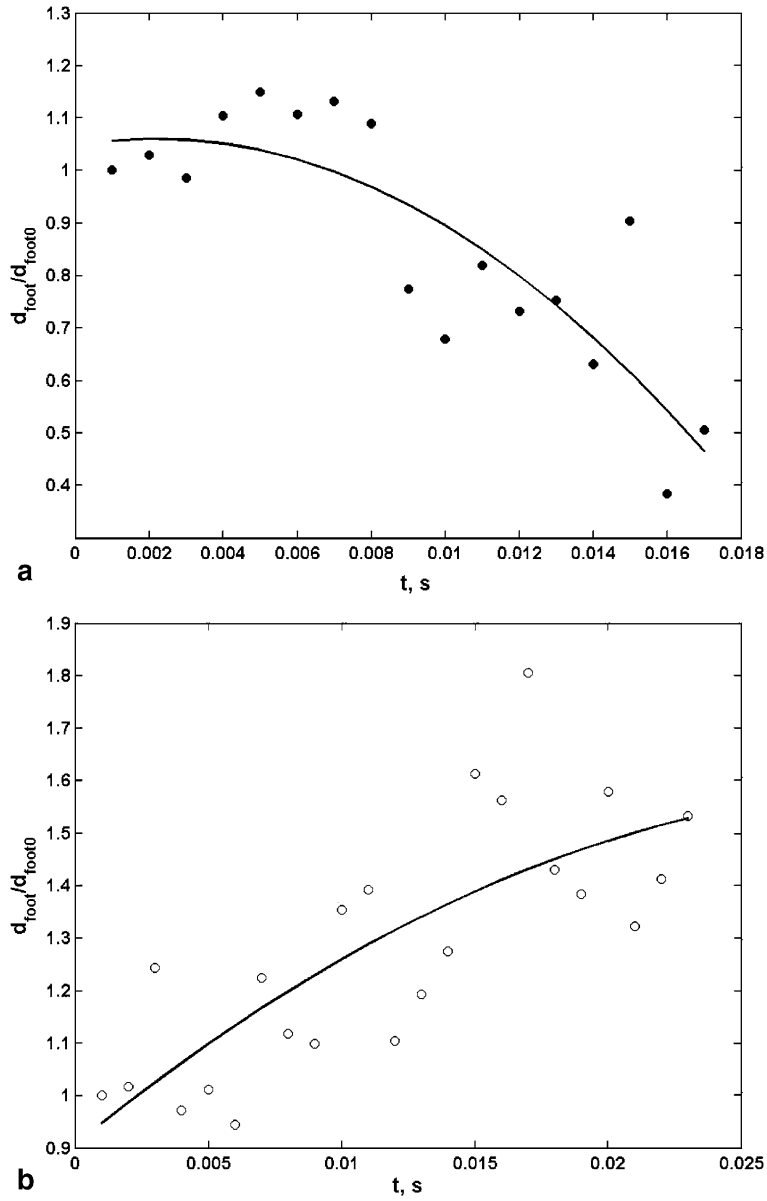


Fig. 12. Ratio $d_{foot}/d_{foot0}$, $q = 10\ kW/m^2$: (a) water, (b) alkyl (8–16).

time, and during period $t = 0.005$–$0.24$ s it decreases in time. The behavior of the contact angle of bubble growth in surfactant solution, at $q = 50\ kW/m^2$, is not presented due to the difficulties of the measurements.

### 3.3. Discussion

The importance of surfactant enhanced boiling is widely recognized and research has been carried out focused in particular on the effect of solubility, surface tension depression, contact angle depression, molecular weight and ionic nature of surfactant on nucleate boiling. In the present study, the bubble dynamics of water and surfactant solution is different, depending on the heat flux.

For some kind of surfactants, when the heat flux reached certain value, the boiling curve of surfactant solution departs from that of water. Boiling curve obtained by Hetsroni et al. (2004a) under conditions of satu-

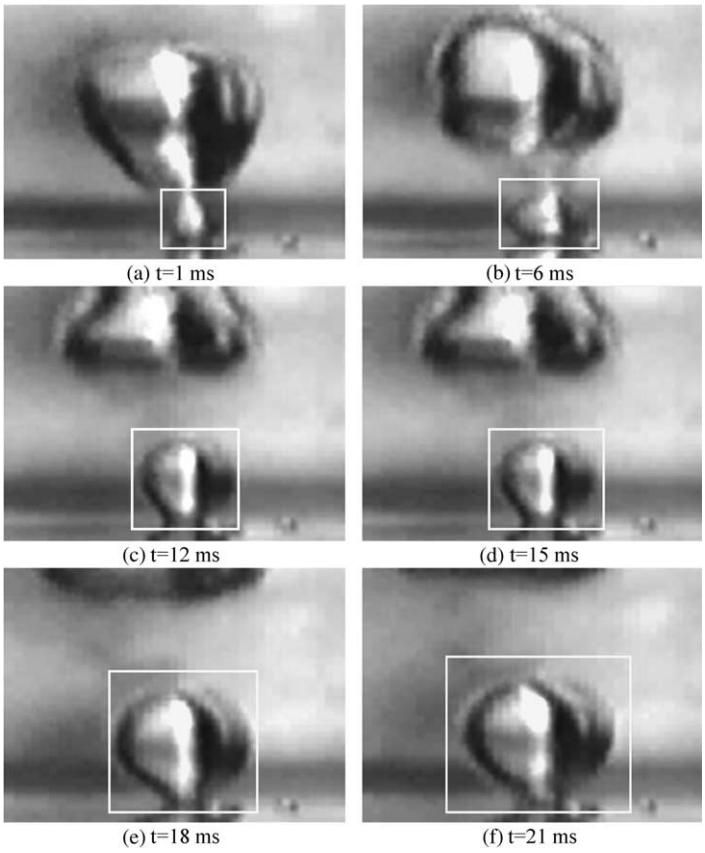


Fig. 13. Boiling of water, $q = 50\ \mathrm{kW/m^2}$.

rated pool boiling of a 600 ppm non-ionic alkyl 8–16 Glycoside surfactant solution has exhibited an S-shape curve. Such a behavior was reported in some previous experimental results (see, for example, Hetsroni et al., 2001).

Some of the mechanisms to elucidate the effect of heat flux and concentration of the solution on the behavior of the boiling curve have been proposed by Sher and Hetsroni (2002). The authors developed a model of nucleate pool boiling with surfactants additives. Solid–liquid and liquid–vapor surface tensions were postulated to be surfactant diffusion controlled. Expressions for them as functions of surfactant bulk concentration and the heat flux were obtained from basic equations. Using those expressions in the nucleate pool boiling correlation, they were able to obtain an explicit expression for the boiling curve, which reproduced the S-shape behavior under certain circumstances. The model was successfully compared to experimental boiling curves obtained by Hetsroni et al. (2001) for pool boiling of a cationic surfactant. Some of the features suggested by this model are supported by the present study. The model postulated the surfactant additives to adsorb to two interfaces: the liquid–vapor and the solid–liquid. Adsorption of surfactant to the liquid–vapor interface decreases liquid–vapor surface tension (as evident from the Gibbs–Duhem equation). The adsorption mechanism of surfactant to the solid–liquid interface was concluded to be through the surfactant's hydrophilic group. In the present study, boiling was generated on a metallic heater with an Alkyl–Poly–Glucoside surfactant, which is a poly-ol surfactant (a surfactant with hydroxyl groups). Being a heated metal, the heater is a slightly negatively charged, hydrophilic surface. Therefore it is postulated that the adsorbed surfactant at the solid–liquid interface is attached to the solid metal with its hydrophilic group, through an electrostatic attraction of the hydrogen of its dipole hydroxyl units. As a consequence, hydrophobic groups of surfactant are in contact with the liquid at the solid–liquid interface, instead of the hydrophilic metal below them. This effect should increase solid–liquid surface tension. Therefore, the surfactant affects the two surface tensions in an

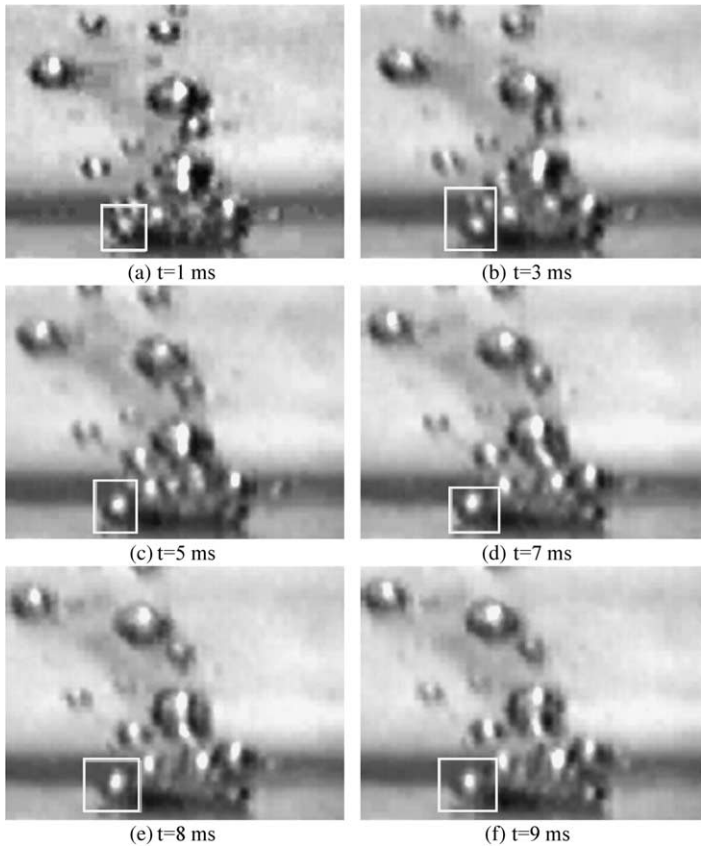


Fig. 14. Boiling of alkyl (8–16), $q = 50\ \mathrm{kW/m^2}$.

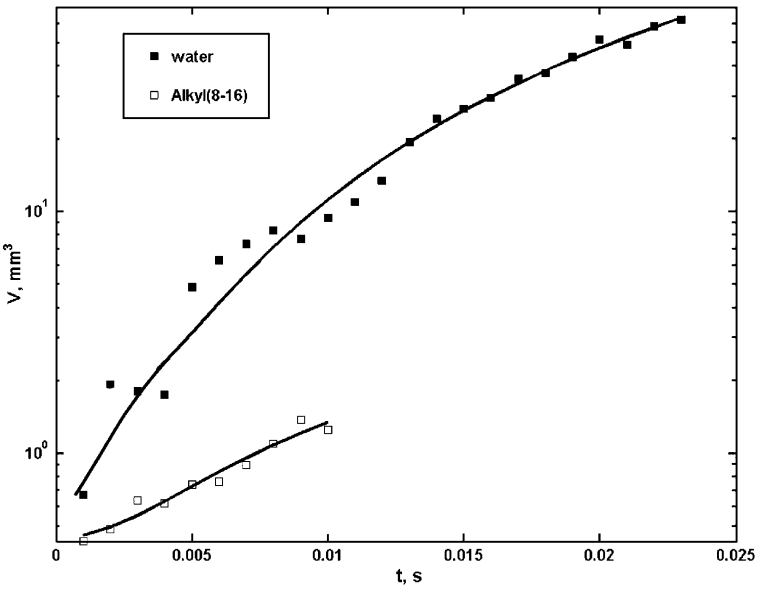


Fig. 15. Dependence of bubble volume on time, $q = 50\ \mathrm{kW/m^2}$.

opposite manner, e.g., decreases liquid–vapor surface tension and increases solid–liquid surface tension. Lowered liquid–vapor surface tension enhances boiling heat transfer by decreasing bubble departure diameter,

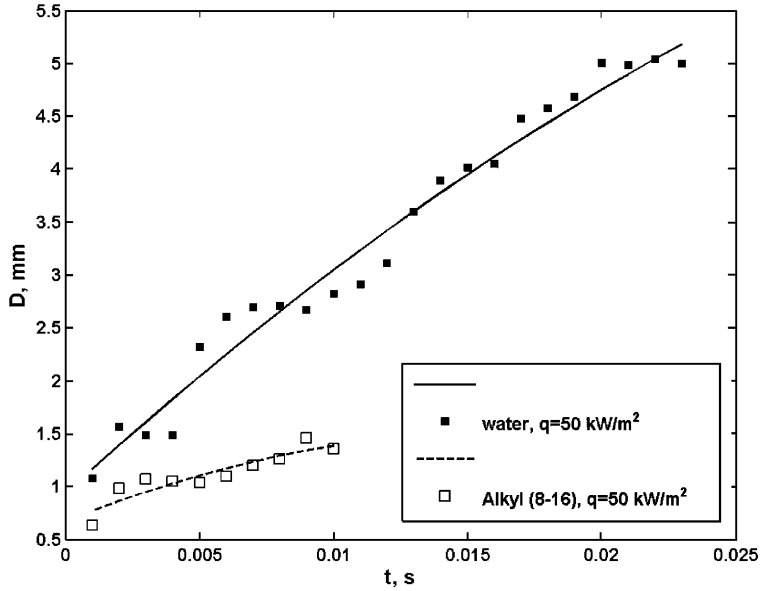


Fig. 16. Time variation of bubble diameter, $q = 50\ \mathrm{kW/m^2}$.

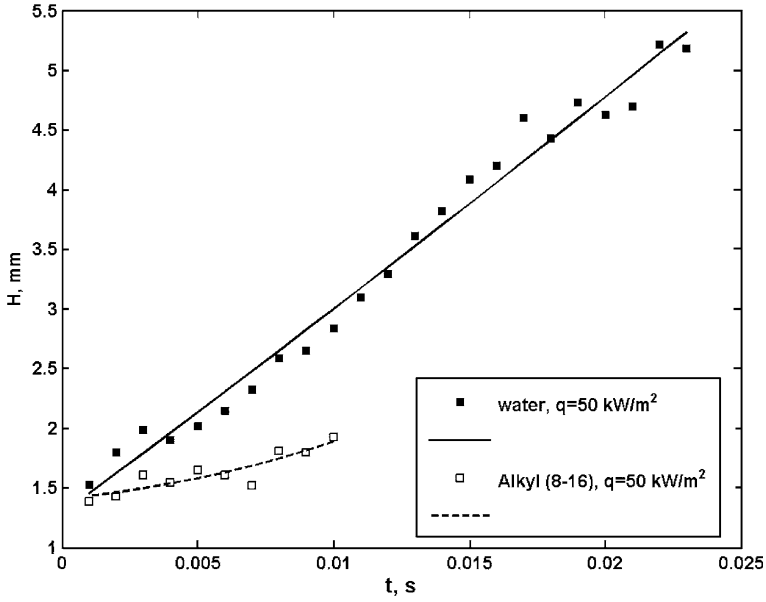


Fig. 17. Time variation of bubble height, $q = 50\ \mathrm{kW/m^2}$.

while elevated solid–liquid surface tension reduces boiling heat transfer by increasing bubble departure diameter. Since surfactant interfacial adsorption process is based on a diffusion mechanism of surfactant from ambient bulk liquid to the interface, the time period enabled for this process to occur is of paramount importance to the magnitude of the effect. In Sher and Hetsroni (2002) this time period is typically associated with vapor velocity, which is directly related to heat flux. At low heat flux the typical time period for diffusion is large, and both the effects of increased liquid–vapor surface tension and decreased solid–liquid surface tension are pronounced, such that the net effect on bubble departure diameter and heat transfer is cancelled. At higher heat flux, the typical time period for diffusion decreases, and the effect of surfactant on both surface tensions is

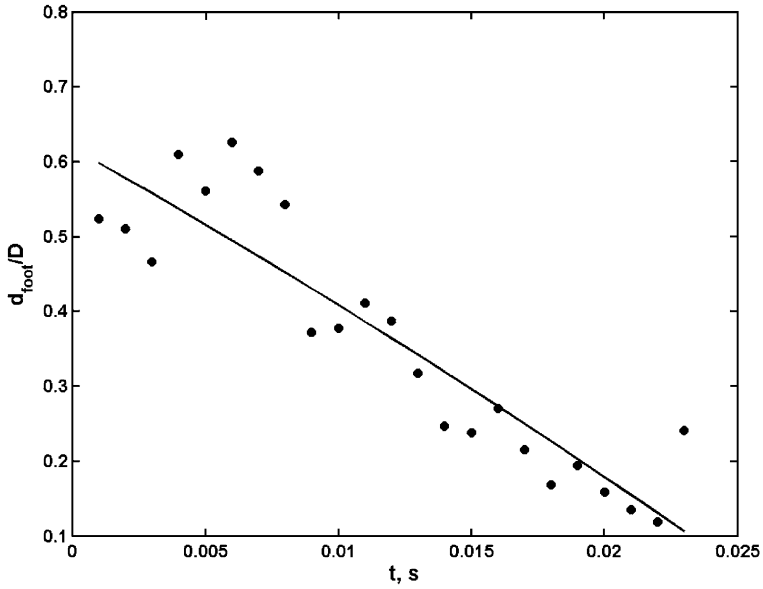


Fig. 18. Time variation of shape parameter, water, $q = 50\ \mathrm{kW/m^2}$.

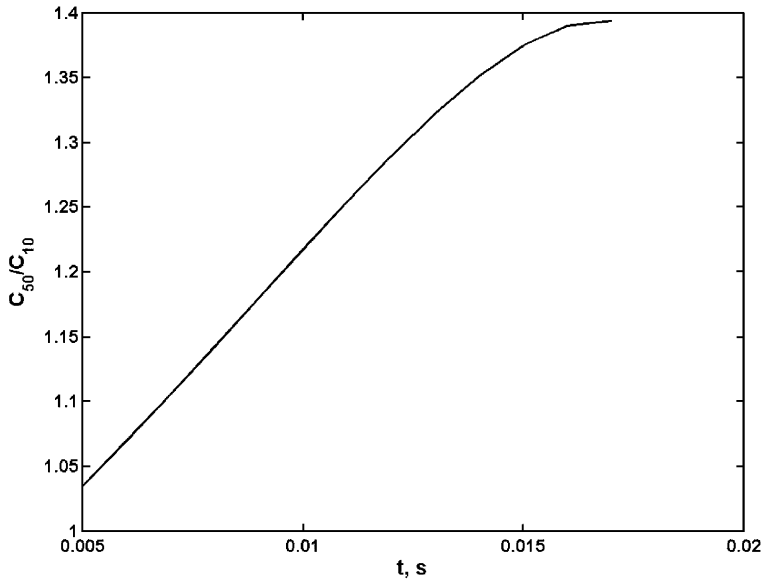


Fig. 19. Time variation of the relation $C_{50}/C_{10}$.

relatively suppressed. Diffusion rate of surfactant to the solid–liquid interface is argued in the model to be smaller than that to the liquid–vapor interface, as to produce a differential suppression between these two effects, such that the net results are a decreased bubble departure diameter and an enhanced heat transfer which are prominent at this heat flux range. At very high heat flux both effects approach a complete suppression of their action. This behavior postulation was shown to generate, in some circumstances, an S-shaped boiling curve. The present study supports some of the postulations of the Sher and Hetsroni (2002) model. At low heat flux ($q = 10\ \mathrm{kW/m^2}$), bubble growth in a surfactant solution did not vary significantly from that in water. A comparison with bubble growth at a higher heat flux ($q = 50\ \mathrm{kW/m^2}$) reveals that while the detach-

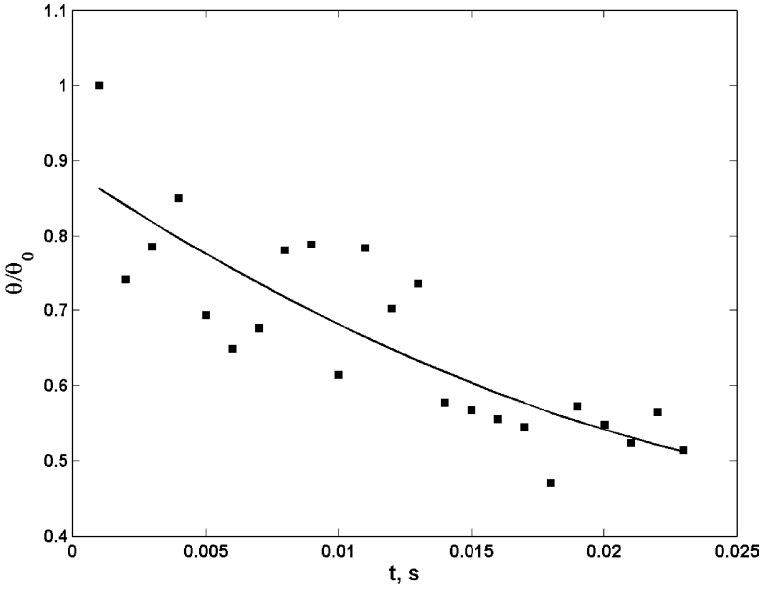


Fig. 20. Time variation of relative contact angle, water, $q = 50\ \mathrm{kW/m^2}$.

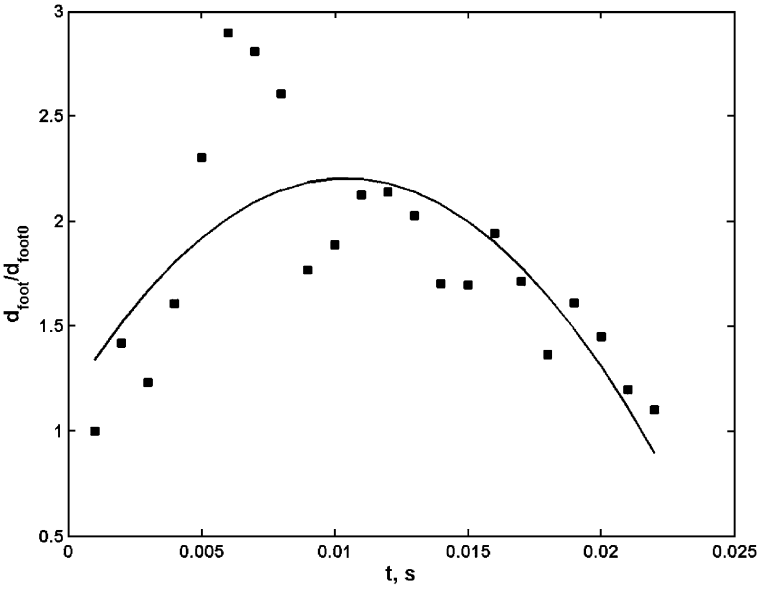


Fig. 21. Ratio $d_{\mathrm{foot}}/d_{\mathrm{foot0}}$, water, $q = 10\ \mathrm{kW/m^2}$.

ment diameter of a bubble in pure water increases with increasing heat flux at this range, the detachment diameter of a bubble in a surfactant solution, decreases with the increased heat flux.

Nucleate boiling in aqueous surfactant solutions is a complex conjugate process, and it depends on a variety of factors. However, the primary heat transfer is by evaporation and its efficiency is directly related to nucleation site density and bubble dynamics. Phenomenological insights can be obtained from a visual observation of water and surfactant boiling at high heat flux. The visualization of bubble growth on a flat surface of water and 600 ppm solution of Alkyl (8–16) Glucoside at $q = 110\ \mathrm{kW/m^2}$ is shown in Fig. 22. A single bubble was formed in water. A different situation arose with the bubble growing in surfactant solution. In comparison to that in water, boiling in surfactant solution was more vigorous and characterized by clusters of small-sized,

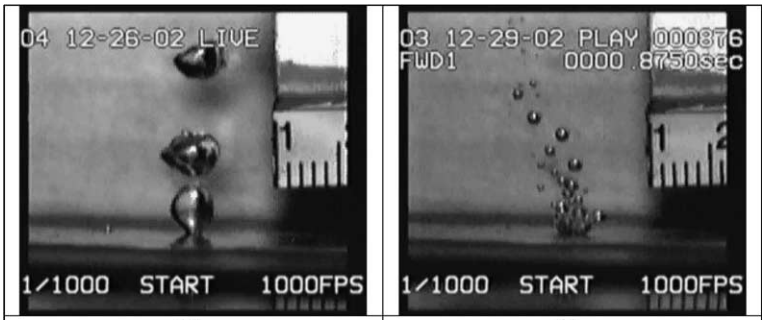


Fig. 22. Boiling on flat surface: (a) water, (b) alkyl (8–16).

more regularly shaped bubbles that had higher departure frequency. One may conclude that surfactant solution promoted activation of a nucleation sites.

Besides the effects discussed above the bulk concentration of surfactant and its chemistry (ionic nature and molecular weight), dynamic surface tension, surface wetting or contact angle, surface adsorption and desorption, dynamic surface tension, and foaming should be considered to have a significant influence. A direct correlation of the heat transfer with suitable descriptive parameters for these effects is difficult due to the complex nature of the problem.

## 4. Conclusions

The bubble growth in a pool boiling in water and non-ionic 600 ppm Alkyl (8–16) surfactant solution was studied using a high speed video. The bubble generation was studied on a horizontal flat surface; the natural roughness of the surface was used to produce the bubbles.

A quantitative analysis for single bubble growth in saturated nucleate pool boiling of water with constant wall heat flux $q = 10$ and 50 kW/m$^2$ was performed. The captured images showed that the bubble shape horizontally is close to axi-symmetric and vertically asymmetric. The time dependence of the bubble volume is $V \sim t^{3/2}$. Throughout bubble growth the contact angle decreases approximately from $\theta = 60°$ up to $\theta = 41°$. The results agree with previous investigations and analytic analyses.

At heat flux of $q = 10$ kW/m$^2$ the shape, life-time and the volume of bubble growth in surfactant solution did not differ significantly from those of water. The time behavior of the contact angle of bubble growing in surfactant solution is qualitatively similar to that of water.

At heat flux of $q = 50$ kW/m$^2$ boiling in surfactant solution, when compared with that in pure water, was observed to be more vigorous. Surfactants promote activation of nucleation sites. The bubbles appeared in clusters. The life-time of each bubble in cluster is shorter than that of a single water bubble. The detachment diameter of water bubbles increase with increasing heat flux, whereas analysis of bubble growth in surfactant solution reveals the opposite effect: the detachment diameter of the bubble decreases with increasing heat flux.

## Acknowledgements

This research was supported by the Fund for the Promotion of Research at the Technion. A. Mosyak is supported by a joint grant from the Center for Absorption in Science of the Ministry of Immigrant Absorption and the Committee for Planning and Budgeting of the Council for Higher Education under the framework of the KAMEA program.

## Appendix A. Determination of bubble parameters

The parameters of the bubble, calculated in the present study, are shown in Fig. A.1a, where $D$ is the maximum diameter of the bubble, $H$ is the height, $V$ is the volume, $d_{\text{foot}}$ is the diameter of the bubble foot, $\theta$ is the

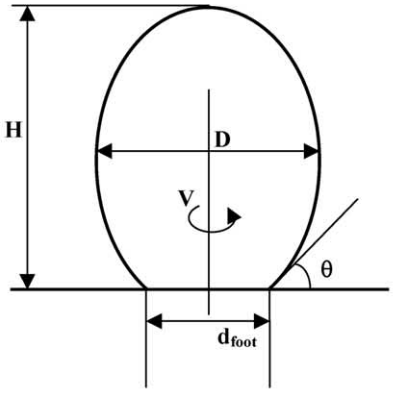


(a)

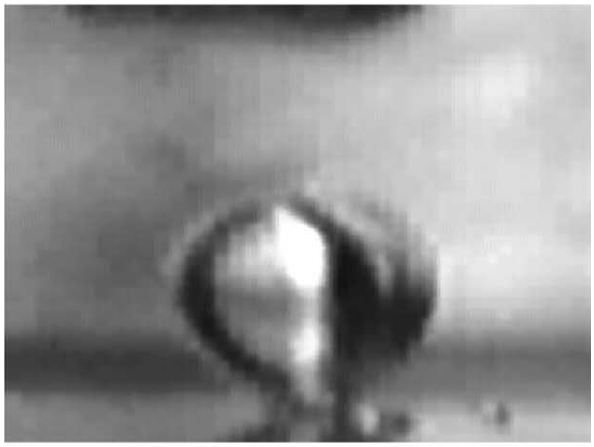

(b)

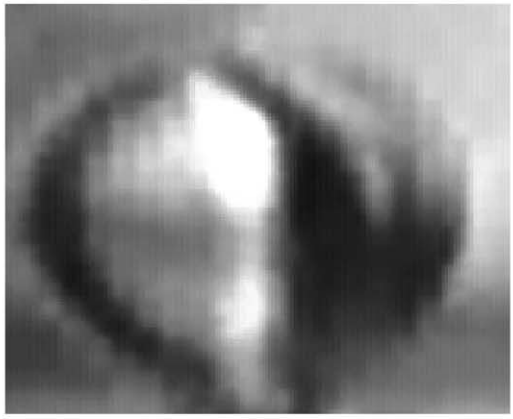

(c)

Fig. A.1. Single bubble: (a) bubble parameters, (b) actual frame from video, (c) cropped bubble image.

contact angle. The growth of bubbles and the bubble motion near the heated surface were recorded by a high-speed video camera as a series of frames. One of the frames from this series (the frame taken from Fig. 13f) is shown in Fig. A.1b. The bubble parameters in each frame of the digitized video were obtained using a code, written in Matlab. For this purpose the edge of the bubble in each frame was detected. The bubble was cropped from the frame to simplify detecting of its edge (Fig. A.1c). We employ the Canny method with

specified sensitivity thresholds. It is more likely to detect true weak edges. It finds edges by looking for local maxima of the gradient of intensity image. The gradient is calculated using the derivative of a Gaussian filter. The method uses two thresholds, to detect strong and weak edges, and includes the weak edges in the output only if they are connected to strong edges. The edge of the actual bubble in the $x$–$y$ plane is shown in Fig. A.2a. The discrete points of these edges were approximated as functions $X_1(y)$ and $X_2(y)$ for the left and the right branches. These branches are shown in Fig. A.2b. Assuming that the bubble is axi-symmetric, its edge $X(y)$ were calculated as the average values of $X_1(y)$ and $-X_2(y)$. This edge is shown in Fig. A.2c.

Fig. A.3 shows the deviation $S = 100 \cdot |d_{2i} - d_{1i}|/d_{1i}$ of the dimensions of the assumed axi-symmetric bubble from those of the actual bubble, where $d_{1i}$ and $d_{2i}$ are the distances between the edges of the axi-symmetric and actual bubble at the same $y_i$ coordinate, $i$ is an index of the given value of $y_i$. The maximum deviation, $S \approx 9\%$

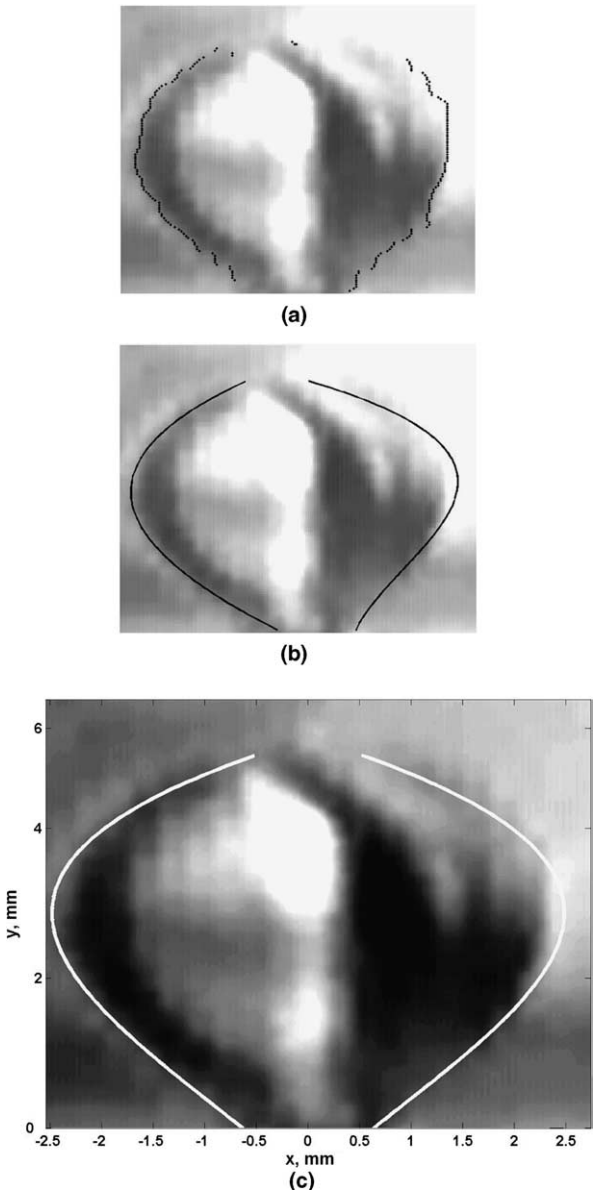


Fig. A.2. Bubble edge: (a) edge obtained using Matlab Program, (b) calculated edge for actual bubble image, (c) symmetric bubble edge (white line).

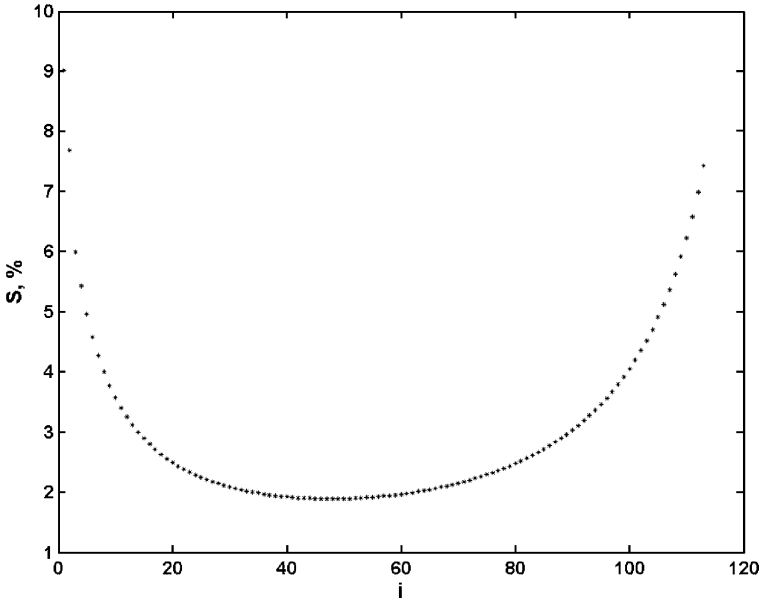


Fig. A.3. Deviation between the actual and assumed dimensions.

was obtained at $i = 1$. This point corresponds to the foot of the bubble. The bubble parameters were calculated as follows: $D = 2 \cdot X_{\max}(y)$, $H = y_{\max}$, $d_{\text{foot}} = 2 \cdot X(0)$, $V = \pi \int_0^H X^2(y)\,\mathrm{d}y$, $\theta = \operatorname{arcctg}(X'(0))$.

## References

Cole, R., Shulman, H.L., 1966. Bubble growth rates at high Jacob numbers. Int. J. Heat Mass Transfer 9, 1377–1390.

Fritz, W., Ende, W., 1936. Uber den verdam-pfungsvorgang nach kinematographischen aufnahmen an dampflasen. Phys. Zeitschr. 37, 391–401.

Geld, C., 2004. Prediction of dynamic contact angle histories of a bubble growing at a wall. Int. J. Heat Fluid Flow 25, 74–80.

Han, C.H., Griffith, P., 1965. The mechanism of heat transfer in nucleate pool boiling- Part I Bubble initiation, growth and departure. Int. J. Heat Mass Transfer 8, 887–904.

Helden, W., Geld, C., Boot, P., 1995. Forces on bubbles growing and detaching in flow along a vertical wall. Int. J. Heat Mass Transfer 38, 2075–2088.

Hetsroni, G., Gurevich, M., Mosyak, A., Rozenblit, R., Segal, Z., 2004a. Boiling enhancement with environmentally acceptable surfactants. Int. J. Heat Fluid Flow 25, 841–848.

Hetsroni, G., Zakin, J.L., Gurevich, M., Mosyak, A., Pogrebnyak, E., Rozenblit, R., 2004b. Saturated flow boiling heat transfer of environmentally acceptable surfactants. Int. J. Multiphase Flow 30, 717–734.

Hetsroni, G., Zakin, J.L., Lin, Z., Mosyak, A., Pancallo, E.A., Rozenblit, R., 2001. The effect of surfactants on bubble growth, wall thermal patterns and heat transfer in pool boiling. Int. J. Heat Mass Transfer 44, 485–497.

Hsu, Y.Y., Graham, R.W. (1961). An analytical and experimental study of the thermal boundary layer and ebullition cycle in nucleate bouling. Nasa TN-D-594.

Klausner, J.F., Mei, R., Bernard, D., Zeng, L., 1993. Vapor bubble departure in forced convection boiling. Int. J. Heat Mass Transfer 36, 651–661.

Kotchaphakdee, P., Williams, M.C., 1970. Enhancement of nucleate pool boiling with polymeric additives. Int. J. Heat Mass Transfer 13, 835–848.

Lee, H.C., Oh, B.D., Bae, S.W., Kim, M.H., 2003. Single bubble growth in saturated pool boiling on a constant wall temperature surface. Int. J. Multiphase Flow 29, 1857–1874.

Manglik, R.M., Wasekar, V.M., Zhang, J., 2001. Dynamic and equilibrium surface tension of aqueous surfactant and polymeric solutions. Exp. Thermal Fluid Sci. 25, 55–64.

Mei, R., Chen, W., Klausner, J.F., 1995a. Vapor bubble growth in heterogeneous boiling. Int. J. Heat Mass Transfer 38, 909–919.

Mei, R., Chen, W., Klausner, J.F., 1995b. Vapor bubble growth in heterogeneous boiling. Part I: Growth rate and thermal fields. Int. J. Heat Mass Transfer 38, 921–934.

Mikic, B.B., Rohsenow, W.M., Griffith, P., 1970. On bubble growth rates. Int. J. Heat Mass Transfer 13, 657–666.

Paul, D.D., Abdel-Khalik, S.I., 1984. Saturated nucleate pool boiling bubble dynamics in aqueous drag-reducing polymer solutions. Int. J. Heat Mass Transfer 27, 2426–2428.

Plesset, M.S., Zwick, S.A., 1954. The growth of vapor bubbles in superheated fluids. J. Appl. Phys. 25, 474–478.
Prodanovic, V., Fraser, D., Salcudean, M., 2002. On transition from partial to fully developed subcooled flow boiling. Int. J. Heat Mass Transfer 45, 4727–4738.
Robinson, A.J., Judd, R.L., 2001. Bubble growth in a uniform and spatially distributed temperature field. Int. J. Heat Mass Transfer 44, 2699–2710.
Rosen, M.J., 1989. Surfactants and Interfacial Phenomena, second ed. Wiley, New York.
Rybinski, W., Hill, K., 1998. Alkyl polyglycosides—properties and applications of a new class of surfactants. Angew. Chem., Int. Ed. 37, 1328–1345.
Sher, I., Hetsroni, G., 2002. An analytical model for nucleate pool boiling with surfactant additives. Int. J. Multiphase Flow 28, 699–706.
Shulman, Z.P., Levitsky, S.P., 1996. Growth of vapor bubbles in boiling polymer solutions-I. Rheological and diffusional effects. Int. J. Heat Mass Transfer 39, 631–638.
Staniszewski, B.E. (1959). Nucleate boiling bubble growth and departure. M.I.T. DSR Project No. 7- 7673, Technical Report No. 16.
Thorncroft, G.E., Klausner, J.F., Mei, R., 1998. An experimental investigation of bubble growth and detachment in vertical upflow and downflow boiling. Int. J. Heat Mass Transfer 41, 3857–3871.
Thorncroft, G.E., Klausner, J.F., Mei, R., 2001. Bubble forces and detachment models. Multiphase Sci. Technol. 13, 35–76.
Van Stralen, S.J.D., 1966. The mechanism of nucleate boiling in pure liquids and in binary mixtures. Int. J. Heat Mass Transfer 9, 995–1046.
Wasekar, V.M., Manglik, R.M., 1999. A review of enhanced heat transfer in nucleate pool boiling of aqueous surfactant and polymeric solutions. Enhanced Heat Transfer 6, 135–150.
Wasekar, V.M., Manglik, R.M., 2000. Pool boiling heat transfer in aqueous solutions of an anionic surfactant. Trans. ASME J. Heat Transfer 122, 708–715.
Wu, W.T., Yang, Y.M., 1992. Enhanced boiling heat transfer by surfactant additives. In: Proc. Eng. Foundation Conf. on Pool and External Flow Boiling. Santa Barbara, California, pp. 361–366.
Yang, Y.M., Maa, J.R., 2003. Boiling heat transfer enhancement by surfactant additives. In: Proc. of the 5th Int. Conf. Boiling Heat Transfer, ICBHT, Montego Bay, Jamaica, May 4–8, 2003.
Zeng, L.Z., Klausner, J.F., Mei, R., 1993. A unified model for the prediction of bubble detachment diameters in boiling system. Part I: Pool boiling. Int. J. Heat Mass Transfer 36, 2261–2270.
Zhang, J., Manglik, R.M., 2004. Effect of ethoxylation and molecular weight of cationic surfactants on nucleate boiling in aqueous solutions. Int. J. Heat Mass Transfer 126, 34–42.
Zuber, N., 1961. The dynamics of vapor bubbles in nonuniform temperature fields. Int. J. Heat Mass Transfer 2, 83–98.